Proceedings of Ninth World Conference on Earthquake Engineering
August 2-9, 1988, Tokyo-Kyoto, JAPAN (Vol.VI)

10-1-10

STUDY ON EFFECT OF VERTICAL GROUND MOTION ON STABILITY OF FILL DAMS

Shunzo OKAMOTO , Choshiro TAMURA ,
Katsuyuki KATO , and DONG Jun

Institute of Industrial Science, University of Tokyo
Minato-ku, Tokyo, Japan

SUMMARY

Earthquake response of an actual earth dam in the vertical direction, vibration failure tests on embankment dam models which are excited horizontally and vertically, simulteneously, and numerical analyses of a stability of the dam models, are presented. From these studies, it is clarified that the influence of the vertical acceleration on the stability of the model is fairly small compared with that of the horizontal one and is considered to be independent from that of the horizontal one, different from the assumption for the ordinal seismic coefficient design method.

INTRODUCTION

Strong ground motions in the vertical direction are often observed at epicentralareas and their vicinities. The maximum accelerations of these motions frequently reach the levels of maximum accelerations in the horizontal direction. This study is of the influences on stability during earthquake of fill dams exerted by horizontal and vertical motions acting at the ground surface simultaneously, examined by earthquake observation results, model vibration failure test results, and numerical analyses. As a consequence, it was learned that the influence of vertical-direction seismic force on stability of a fill dam is small compared with that in the horizontal direction, and that the two forces can be considered to be independent of each other.

EARTHQUAKE RESPONSE IN VERTICAL DIRECTION OF ACTUAL FILL DAM

Recently, earthquake observations have come to be carried out at many large dams, and the actual behaviors are beginning to be brought to light. The authors have been making earthquake observations at Sannokai Dam (center-core type earth dam, height 37 m, crest length 145 m, upstream slope gradient 1:2.9, downstream slope gradient 1:2.6 (average)) since 1963. Accelerograph-type strong-motion seismometers are installed at the center and right and left banks (on bedrock) of the dam crest, and at the downstream slope. According to observations, when tremors are not strong, the fundamental frequency is 2.8 Hz for vibrations in a direction orthogonal to the horizontal dam axis, while the secondary natural frequency is 2.9 Hz in the horizontal dam-axis direction, the predominent vibration in the vertical direction being 4.1 Hz. The fundamental frequency, in an earthquake where maximum acceleration on bedrock reached 55 gal in the horizontal direction, was seen to decline to 2.4 Hz. The bedrock incidentally is mainly green tuff with a part being lava.

Figs. 1 and 2, respectively show the maximum accelerations at the crest and bedrock in the direction orthogonal to the horizontal dam axis and in the vertical direction, the abscissa showing data from on the bedrock. From these figures, it can be seen that the maximum acceleration in the vertical direction at the dam crest is approximately 1/2 of that in the direction orthogonal to the horizontal dam axis, and that both are not proportionate to the maximum acceleration of the basement but to approximately the 0.85 power to indicate a nonlinear property. It may be comprehended from this that it will be necessary for an appropriate correlation to be made in evaluation and design of aseismic strength with regard also to the earthquake response in the vertical direction of a fill dam.

MODEL VIBRATION FAILURE EXPERIMENTS

As shown in Fig. 3, a three-dimensional model 60 cm in height was built on the concrete model of the valley on a shaking table, and in a hollow condition this was made to fail applying sine waves of constant frequency (8 Hz). The gradients of the upstream and downstream slopes of the model were the same, being between 1:1.6 and 1:2.2. The material for the model was Onahama sand (specific gravity 2.71, D_{10} = 0.14 mm, D_{50} = 0.76 mm, U_C = 1.32) and slight compaction was done dropping a wooden block from a height of 10 cm from the surface. Since moisture content would greatly affect cohesion, it was carefully controlled and measured. The mechanical properties of the material were tested in a condition of extremely low restraint to simulate the model test using a double-cell triaxial testing machine. The strain dependencies of stiffness and damping factor are indicated in the numerical analysis in the following section.

The fundamental frequency of this model was from 40 to 45 Hz so that the exciting frequency of 8 Hz was considerably lower in comparison, and the acceleration at the crest was amplified by only about 20 percent of the foundation until close to failure of the model.

Fig. 4 shows the slip lines of the cross section plotted upon exciting at the same phase from the two directions of vertical and horizontal. The figure (a) shows the slip lines when causing failure on increasing acceleration while maintaining the ratio (V/H) of vertical acceleration (V) and horizontal acceleration (H) at 0, 0.51, 0.83, and 1.0. The slope gradient was 1:1.6. As the ratio (V/H) increased, slipping occurred deeper from the surface. The figure (b) shows the case for slope gradient of 1:2.2, and the same trend as in (a) can be recognized, but the point that differs from (a) is that the slip line cannot be simulated with a simple, single-arc curve. This occurs when the slope gradient becomes gentle. The acceleration of the shaking table when the model fails (hereafter called "failure acceleration") increases.

Fig. 5 shows failure accelerations with gradient and moisture content of the model as parameters. The abscissa and the ordinate respectively indicate horizontal and vertical accelerations. With slope gradient and moisture content constant, it can be seen that the relationships may be expressed by almost parallel straight lines. According to this, the influence of vertical acceleration on failure is approximately 1/3 that of horizontal acceleration.

Fig. 6 shows the curves at failure in cases of phase differences between vibration waveforms in the two directions and exciting in a manner that so-called elliptical resurge curves would be indicated. The straight line in the figure is the straight line of the failure acceleration obtained from moisture content and slope gradient of the model according to the relationship, and it can be seen that the straight line may be considered as being in contact with the ellipses.

NUMERICAL ANALYSIS

Response calculations were made in order to analyze the results of the experiments described in the preceding section. The model made the study subject was a two-dimensional one with a height of 60 cm and gradient of 1:2.2, anchored on bedrock. The stiffness and damping factor of the material are as shown in Figs. 7 and 8, the density being 1.47 gr/cm^3 and the Poisson's ratio 0.3. The

time history was calculated by the finite element method. The equivalent linearization method was used, the meshes being as shown in Fig. 9. An example of principal stress distribution is shown in Fig. 10. The dead weight has been included in the calculation process. It is noted that the stresses in Fig. 10 are correspond to the acceleration direction of the shaking table shown in the figure, because the slope of the dam model slides down under this condition.

As Fig. 4 shows, the slip lines are approximately parallel to the slope, and so the following calculation were made for the four points of 1 to 4 given in Fig. 9.

A. The normal stress (σ_n) and shear stress (τ) at the surface element parallel to the slope are obtained for each of the points. This is done for the case of excitation in the horizontal direction only and the cases of exciting in the vertical direction with 200 gal or 400 gal while exciting in the horizontal direction with 400 gal. The two excitation waveforms were same in phase.

B The frictional resistance (τ_f) is calculated from normal stress (σ_n), provided that the angle of internal friction ϕ is taken as 39 deg from test results.

$$\tau_f = \sigma_n \tan \phi \qquad (1)$$

The values of τ and τ_f determined in this manner are shown in Figs. 11 and 12.

CONSIDERATIONS

As stated under Model Vibration Failure Experiments, it was found that within the scope of the experiments the influence of ground motion in the vertical direction was approximately 1/3 compared with ground motion in the horizontal direction. Therefore, this was confirmed from the results of the numerical analyses of the preceding section.

As shown in Figl 11, when exciting in the horizontal direction only, by increasing acceleration by 100 gal, τ_f is decreased by 0.40 gf/cm^2 while τ is increased by 0.90 grf/cm^2, and the condition is that there is a tendency to slip by a total of 1.30 grf/cm^2. According to Fig. 12, when acceleration is increased 100 gal in the vertical direction, τ_f is decreased 0.83 grf/cm^2 while τ is also decreased 0.40 grf/cm^2, so that the condition would be for a tendency to slip by 0.43 grf/cm^2 (= 0.83 - 0.40). Therefore, acceleration in the vertical direction will have an influence of approximately 1/3 (0.43/1.30) of that in the horizontal direction. This is also the same when the mechanical characteristics of the material are linear. This value coincides with that from experimental results.

As shown in Fig. 13, when the axis for stability evaluation is considered and the acceleration on this axis is taken to be a stable acceleration (A_S), it can be expressed by the following equation:

$$A_S = A_H \cos \theta + A_V \sin \theta \qquad (2)$$

where, A_H is horizontal acceleration, and A_V is vertical acceleration. The value of A_S is determined by the slope gradient and physical properties of the material. As shown in Fig. 6, in the case that there is a phase difference (α) between A_H and A_V, A_S can be expressed by the following equation:

$$A_S = \sqrt{(A_H \cos\theta + A_V \sin\theta)^2 - 2A_H A_V \sin 2\theta \sin^2(\alpha/2)} \qquad (3)$$

When A_S in equation (2) is transformed into equivalent horizontal acceleration,

$$\frac{A_S}{\cos \theta} = A_S' = A_H + A_V \tan \theta \qquad (4)$$

Since θ also may be considered as a constant for each dam, in case the accelera-

tions of A_H and A_V act simultaneously, it may be considered from Eq. (4) as being equivalent to the case of action of horizontal acceleration of A_S'.

The conventional resultant seismic coefficient may be expressed by the following equation:

$$\left.\begin{aligned} K_H' &= \frac{K_H}{1 - K_V} \\ \text{or } K_H &= K_H' (1 - K_V) \qquad (1 - K_V > 0) \end{aligned}\right\} \qquad (5)$$

When considered with A_S', A_H, and A_V correlated respectively with K_H', K_H, and K_V in Eqs. (4) and (5), in Eq. (5) the coefficient of K_V is K_H' and is determined uniquely without becoming a value independent of seismic coefficient. This is contradictory to previous results.

Next, what kind of effect the angle of internal friction (ϕ) will have on θ in Eq. (4) will be considered.

By Eq. (1), τ_f can be calculated for any value of ϕ. When $\phi = 39°$ and the excitation forces increase 100 gal in the vertical and horizontal directions, τ_f and τ are decreased by 0.40 grf/cm^2 and 0.83 grf/cm^2, so that tan θ of Eq. (2) for any ϕ can be obtained by the following equation:

$$\tan\theta = \frac{\text{Increase in tendency to slip under 100 gal in vertical direction}}{\text{Increase in tendency to slip under 100 gal in horizontal direction}} = \frac{-0.40 + 0.83 \dfrac{\tan\theta}{\tan 39°}}{0.90 + 0.40 \dfrac{\tan\theta}{\tan 39°}}$$

Table 1 is thus obtained.

Table 1

ϕ	36°	39°	42°	45°
tan θ	0.24	0.33	0.38	0.45

When ϕ is increased, tan θ will be a large value, but it may be considered that A_S' will increase on the other hand.

On consideration of the observation results described in "Earthquake Response in Vertical Direction of Actual Fill Dam," if there had been ground motions in the horizontal and vertical directions equal to maximum accelerations at the base, it may be considered that the maximum acceleration in the vertical direction will be about 1/2 of that. In this case, from Eq. (4),

$$A_S' = A_H \left(1 + \frac{1}{2} \tan\theta\right) \qquad (6)$$

Consequently, Table 2 is obtained from Table 1.

Table 2

ϕ	36°	39°	42°	45°
A_S'/A_H	1.12	1.17	1.19	1.23

The values in Table 2 are fairly small compared with the values obtained by Eq. (5) for a large value of K_H suggesting that a small value can be taken for the resultant seismic coefficient for design. This is a matter requiring further study.

In closing, the authors wish to thank Messrs. M. Morita, H. Hirai, and S. Okamoto, formerly graduate students of the University of Tokyo, for their cooperation in conducting the experiments in this study.

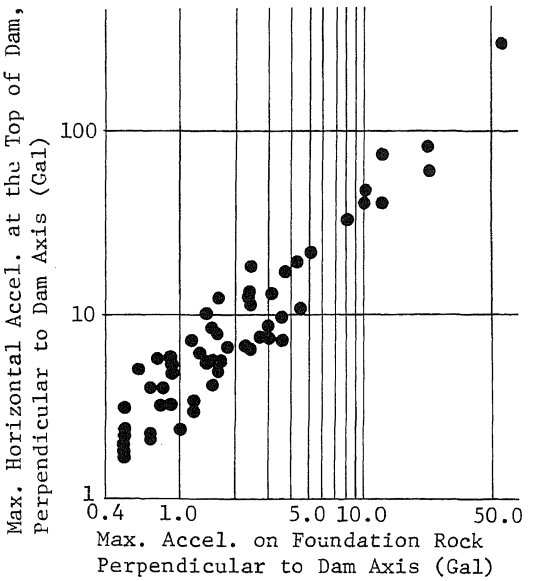

Fig. 1 Max. Accelerations at the Top of Dam and at the Base Rock, Perpendicular to the Dam Axis

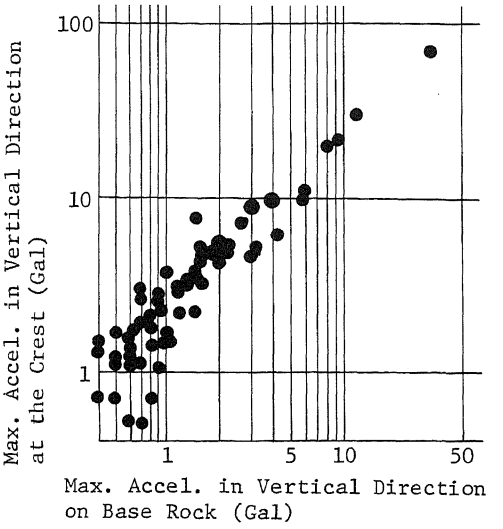

Fig. 2 Max. Accelerations at the Top of Dam and at the Base Rock, in Vertical Direction

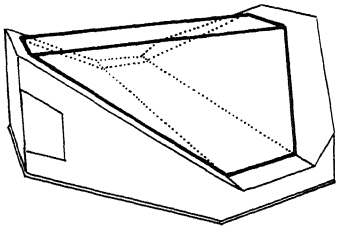

Fig.3 Rough sketch of model

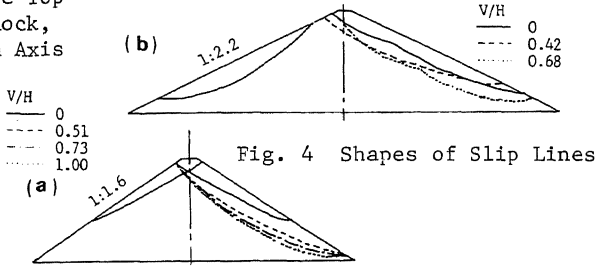

Fig. 4 Shapes of Slip Lines

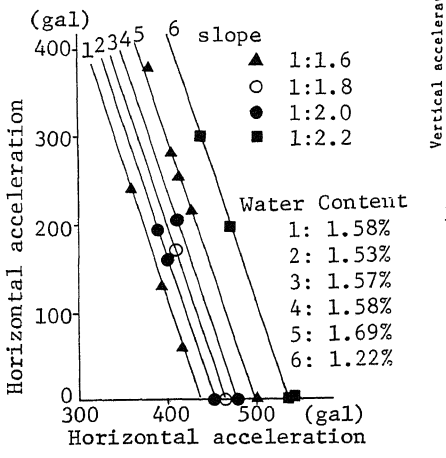

Fig.5 Relationship between horizontal and vertical accelerations at the time of failure of dam models

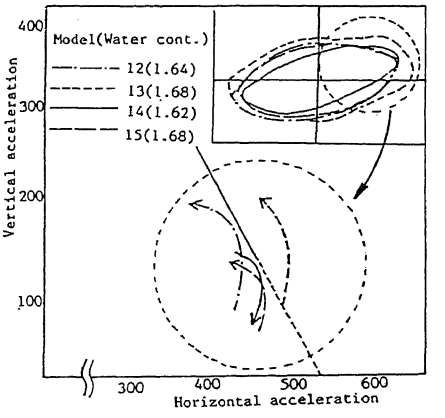

Fig. 6 Elliptical Resurges Curves of Two Accel. Waveforms, Horizontal and Vertical, at Failure Condition

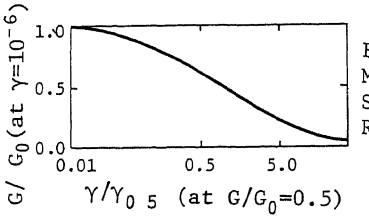

Fig. 7 Shear Modulus G vs. Shear Strain γ Relationship

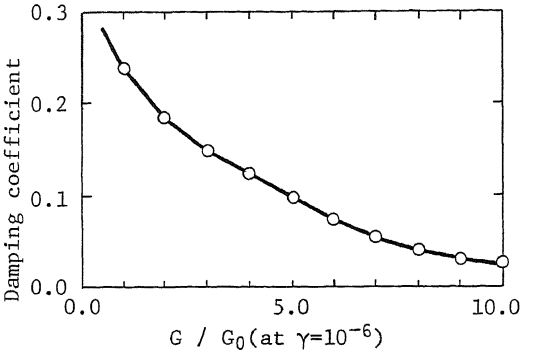

Fig.8 Variation of damping coefficient with shear modulus

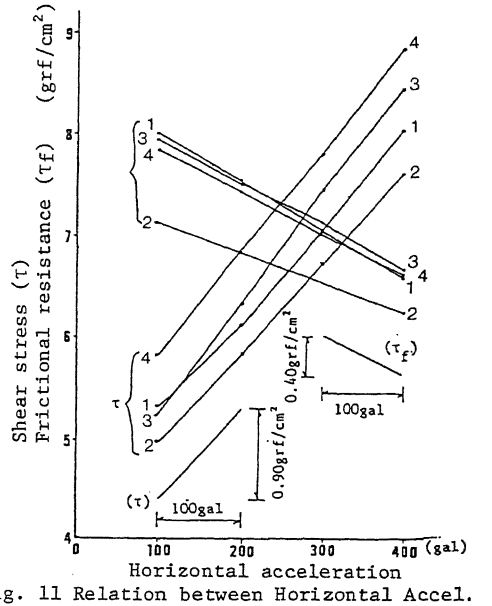

Fig. 11 Relation between Horizontal Accel. and Shear Stress or Frictional Resistance at Points No. 1-No. 4

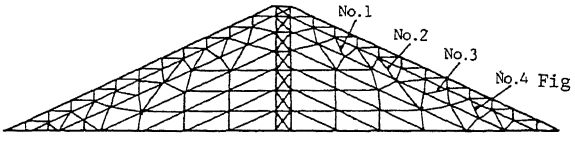

Fig. 9 Mesh for analysis

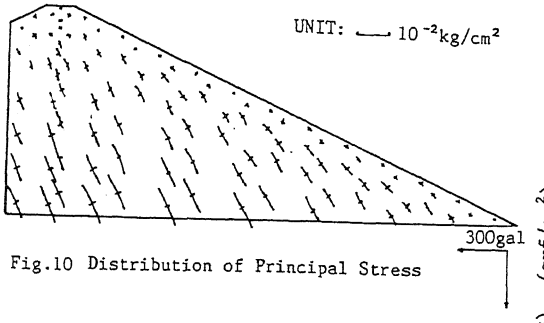

Fig.10 Distribution of Principal Stress

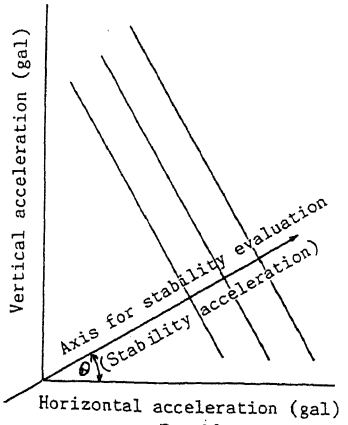

Fig.13
Illustration of new axis for evaluation of stability of dam

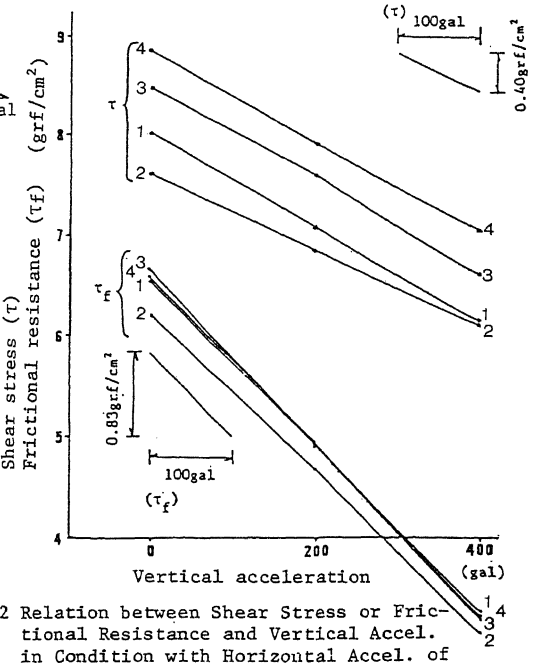

Fig. 12 Relation between Shear Stress or Frictional Resistance and Vertical Accel. in Condition with Horizontal Accel. of 400gal, at Points No.1-No.4